International Journal of Engineering Education Vol. 29, No. 2, pp. 533–547, 2013
Printed in Great Britain

0949-149X/91 $3.00+0.00

Development of a Methodology to Learn the Characteristics and Performances of Common Rail Injection Systems Based on Simulations with AMESim*

R. PAYRI, J. JAVIER LÓPEZ, F. J. SALVADOR and P. MARTÍ-ALDARAVÍ
CMT-Motores Térmicos, Universitat Politècnica de València Camino de Vera s/n, E-46022 Spain. E-mail: fsalvado@mot.upv.es

An injector model built with the platform LMS Imagine.Lab AMESim has been introduced as a useful tool used in one of the practical lessons taught in the "Mixing formation and combustion systems in the Reciprocating Internal Combustion Engines" course. This course carries 6 ECTS and is a first year course in the second semester of the Master's in "Reciprocating Internal Combustion Engines". Using a standard model that has been previously implemented and validated, the students have to carry out an analysis of the injection process from the point of view of the operation of a modern solenoid-valve operated injector. The goal pursued in the lesson described here is, on the one hand, to help the students to understand how injectors work from the moment when they receive the current from the ECU of the engine up to when the fuel is delivered to the combustion chamber as a diesel spray. The different mechanisms involved will be analyzed by the students by exploring important internal variables, such as pressure variations, moving part displacement and, in overall terms, all the variables involved in the injection phenomenon. On the other hand, the students will be able to identify the critical parameters that play a major role, affecting the mass flow rate to a greater extent, by analyzing the response of the system under different geometrical configurations and different operating conditions. There is some evidence that the new teaching approach significantly improves the learning process when compared with the previous teaching methodology.

Keywords: injection modeling; diesel; students; workshop; AMESim

1. Introduction

Currently teachers at engineering schools are facing a tremendous challenge: they have to show their students how today's extremely complex mechanical systems work but take the same (or even less) time and workload in doing so than 20 years ago. This is why research in engineering education has focused on educational technology (on-line, distance, web-based learning...) over the past years [1]. For this purpose, computer simulations introduce a real potential for improving and accelerating the student learning process [2], and students perceive computational simulations as effective learning tools [3]. This is the case, for instance, in modern fuel injection systems used in current automotive engines [4]. They have been developed and introduced in the market (specially in diesel engines) to allow better control of the fuel injection rate, as it has been shown that using multiple injection strategies introduces a significant potential for modifying combustion development and reducing the formation of pollutant [5–7].

Numerous studies have been completed to model the behavior of these last generation hydraulic injection systems [8–14]. The flow modeling is always based on the conservation of momentum and mass. The effect of cavitation and fuel property variations has also been considered in recent works [9, 12–16], which allow more accurate models to be obtained. For example, some papers [16–18] discuss the treatment of the non-linear bulk modulus to include temperature and pressure variations for two phase flow. These recent models also require further modeling of elements that are closely related to the injection system and elements of the electronic control system. From an experimental point of view, it is difficult to obtain information about the internal hydro-dynamic behavior of the system. By using these developed models, if they are sufficiently accurate, information can easily be obtained. Furthermore they make it possible to reproduce injection rates without the use of an injection test bench.

Another important point concerning these models is that they can be used to carry out sensitivity studies [8–10, 13]. This means that the influence on the injection rate can be determined both qualitatively and quantitatively by testing different design parameters such as: volumes, stiffness of springs, control diameter orifices and so on.

The success of obtaining models of injection systems that accurately reproduce reality is based on using methods that produce a good characterization at both a dimensional and a hydraulic level. The term "accurate model" means a model that is able to

* Accepted 22 November 2012.

reproduce the same values for the mass flow rate and injection rate as measured experimentally within real operational ranges. This accurate characterization is a basic necessity for the correct modeling of the injection system, as it produces the input data for the calculation code used for the simulations. The rigor of this characterization, together with the potential of the calculating code, which is able to reproduce physical phenomena and observations, contribute to a more reliable final model.

The choice of a one-dimensional model seems to be the best way to deal with the study of this kind of system because it provides the chance to study the internal hydro-dynamic behavior of the injector, which would otherwise be difficult.

The current practical lesson will be the second one on the topic; the first practical lesson will deal with how to use the software, without any specific objective, and lasts 2 hours. The current practical lesson will be the second lesson and it will comprise a 4 hour class in groups of two. The subject ''Mixture formation and combustion'' is part of the second module of 30 credits (process and technology) and it is structured in four consecutive parts: diesel fuel injection and sprays, gasoline injection, combustion in compression ignition engines and combustion in spark ignition engines. The Master in Reciprocating Internal Combustion Engines has between 12 and 15 new students every year, so up to eight computers with AMESim licenses on them are needed for the current practical lesson.

It is worth underlining that the main contribution of this paper is not the modeling of a common rail fuel injection system, nor the use of computer simulations as a teaching methodology or a learning activity. The actual novelty is the use of computer simulations of a common rail fuel injection system as a powerful tool to allow the student to understand in depth the operation of such a complex system. This teaching methodology can be applied in other engineering fields where other complex systems are also available.

As far as the structure of the paper is concerned, the paper is divided into five sections. First, in Section 2, the description of a one-dimensional model that has been obtained and extensively validated with experimental data will be explained. The model is based on the metrological and hydraulic characterization of a second generation Bosch common rail, which has been explained and validated in [13]. In the present paper, only a review of the main points of the model will be presented in order to make the description of the practical case more understandable. The model of the injector is divided into three parts: injector holder, nozzle and electro-valve. The validation of the model is performed by comparing the mass flow rates provided by the model with those obtained experimentally by means of a mass standard injection rate discharge curve indicator (IRDCI) based on the Bosch method.

In Section 3, the students' work is described. First the simulation matrix where the points to be simulated are defined is described. Then the students have to describe how the injector works by means of an analysis of the injector internal variables such as pressures, control flow, displacements, etc. The influence of the rail pressure on the needle lift laws and velocities is studied and analyzed by the students in the next subsections. The pressure losses and dynamics effects due to pressure waves generated during the injection process are then analyzed. Finally, the effective injection pressure (upstream of the discharge orifices) and the injection velocity (which is the most important parameter involved in the subsequent air–fuel mixing process) are analyzed by the students for the different simulated points.

The final point of this subsection is devoted to the prediction of the mixing and combustion processes of the air–fuel. At this point, the students have to choose which of the different simulated points is expected to have a better performance from the mixing point of view. This reasoning will serve as a link to the next practical lesson where the students study and analyze the spray behavior of the same points simulated here with the help of a phenomenological diesel spray model.

In Section 4, the influence of including the AMESim platform as a methodology on the learning of the subject is evaluated.

Finally, in Section 5, the most important conclusions of the paper presented here are drawn and briefly discussed.

2. Injection system and model description

For the model, a commercial integrated platform for 1D systems simulation, AMESim, was used [19]. Within this platform, a set of validated libraries containing pre-defined components for different physical domains can be used to create a simulation model for the injection system. The components are described using validated analytical models that represent the injection system's actual hydraulic, mechanic and electric-magnetic behavior.

The proposed model for the injector is shown in Fig. 1, where the whole injection system, composed of a pump, a rail, and several lines and injectors, is shown. The most important part of the injection system is the injector, and the practical lesson deals with its operation and analysis.

The model for the injector has been divided into three parts: the injector nozzle, the injector holder

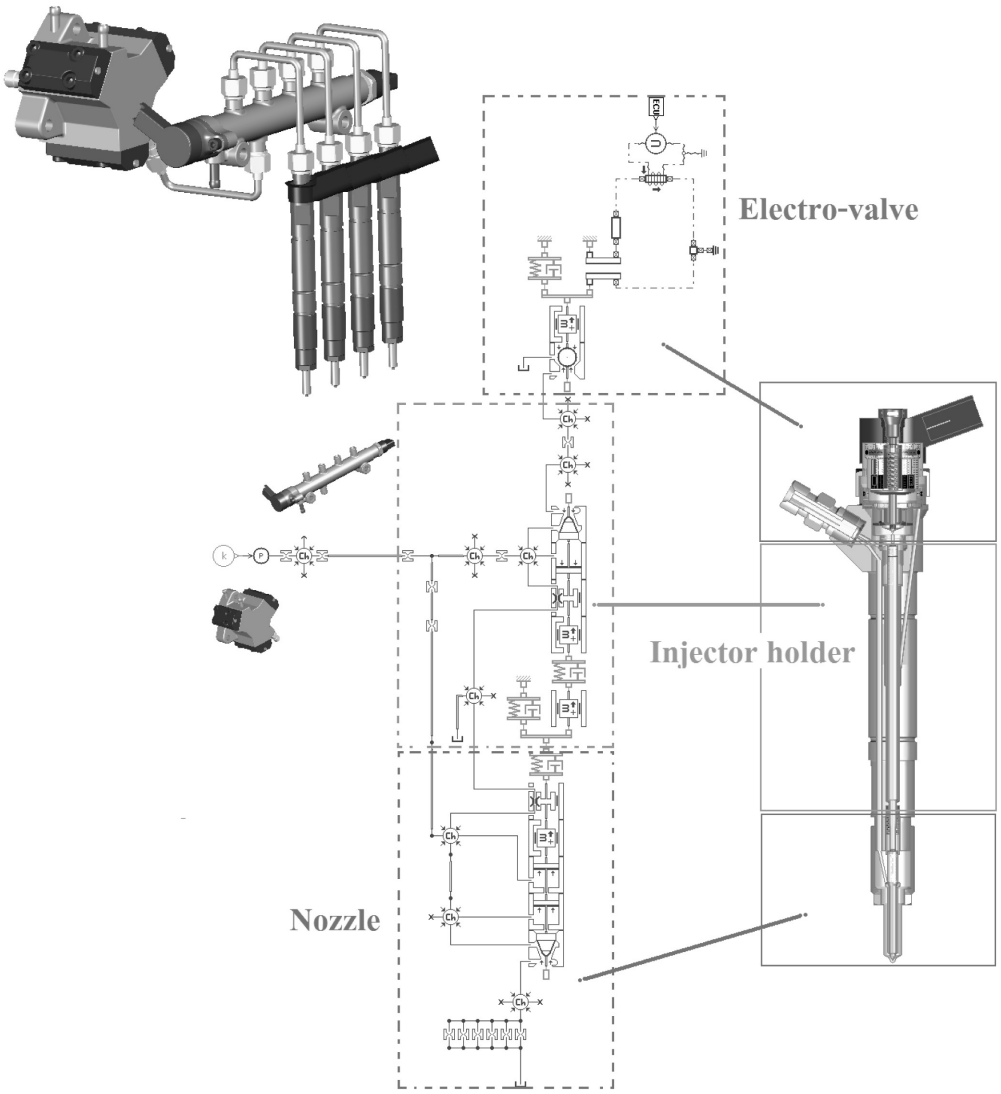

Fig. 1. Global modeling of the fuel injection system (adapted from [13]).

and the electro-valve, all of them connected mechanically and hydraulically, as described in the following subsection.

The proposed methodology for modeling the injection system is based on two different types of characterization: a detailed dimensional characterization and a hydraulic characterization of the different internal parts of the injectors. For the dimensional characterization, an accurate and detailed measuring technique applied to all the internal constituents of the injector is used. It is based on the use of silicone molds of the internal channels and volumes, which are subsequently visualized. The hydraulic characterization makes reference mainly to the characterization of the mass flow rate at different pressure conditions for all the calibrated orifices (either in the nozzle or in the control volume of the injector), which together with the dimensional information allows the discharge coefficient to be determined as a function of the pressure drop. Both types of characterization are explained in depth in [13].

2.1 Model of the injector holder

The proposed model of the injector holder is shown in Fig. 2. In this model a pressure source is considered to be simulating the pump. This pressure source feeds a volume of 20 cm^3, which represents the rail. The rail is connected to the injector holder with a high pressure line (HPL1). At the entrance of the injector holder there is a restriction simulating the edge filter (HPF). Following this, there is a separation into two lines. The first one directly feeds the nozzle (through lines L2, L3 and L4). The second line feeds the upper part of the injector, through volume V1, the control volume inlet orifice (orifice OZ) and, finally, volume V2, where the upper part of the rod is located. The conical section

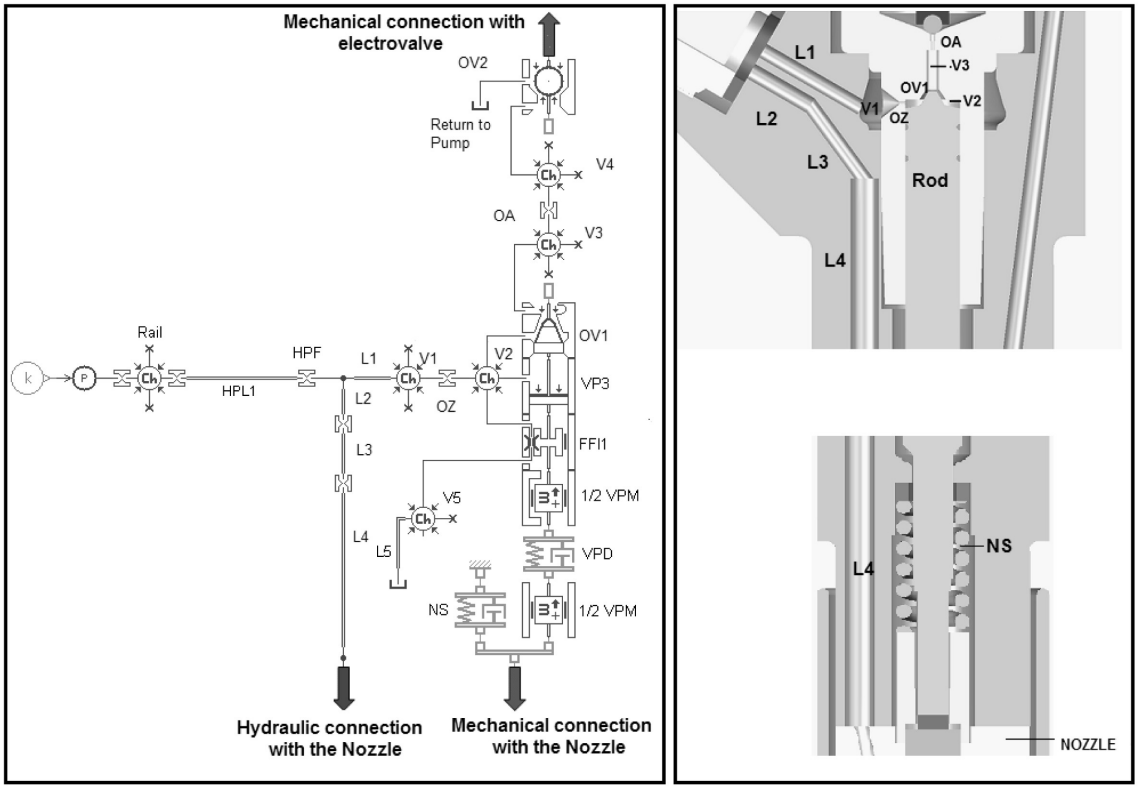

Fig. 2. Model of the injector holder (adapted from [13]).

in the upper part of the rod has been modeled by a conical valve, which fits very well to the actual shape of the upper part of the rod, the effective section of which varies with the rod lift. Moreover, and additional piston that takes into account the pressure force acting on the flat part of the upper section of the rod is considered (VP3). Following the conical valve (OV1), the volume V2 is located, which precedes the control volume outlet orifice (OA), the opening of which is controlled by the command piston of the electro-valve. After this orifice, the return channel is located.

For the characterization of volume 2 and volume 3 (V2 and V3), photographs taken with an electronic microscope from the silicone mold previously mentioned were used. More details about the injector holder model are available in [13].

2.2 Model of the nozzle

In Fig. 3, on the right, a sketch of the nozzle with the different internal lines and volumes is shown. The most important part from the point of view of the model is the configuration of the needle seat. In Fig. 3, on the left, the proposed model of the nozzle is depicted. This model is connected to that of the injector holder by means of a hydraulic connection (NL1) and a mechanical connection (mechanical contact between the needle and the rod). In the upper part of the nozzle the line NL1 can be found, feeding the volume NV1, connected to the piston NP1, which allows the simulation of the action of the pressure force in the upper part of the needle. After the volume NV1 the line NL2 is located, with a section equivalent to the clearance between the needle and the internal part of the nozzle where the needle is placed. This line feeds the volume NV2, associated with the piston NP2, which simulates the volume existing between the needle and its seat, and the crown under the action of pressure force. The volume NV2 also feeds the valve with a conical seat (OV3) simulating the tip of the needle and its seat. Following the conical valve, the volume NV3, connected with the five discharge orifices, is placed.

For the dimensional characterization of all these volumes and the geometrical sections of the different pistons considered in the model, the superposition of a photograph of the needle and a photograph of the silicone mold of the seat (including orifices) was used [13]. The conical seat (OV3) and the two pistons considered are mechanically connected to the needle mass (NM) that, in turn, is connected to a fictitious spring. This spring does not actually exist, but it allows one to model the deformation of the needle that is caused by the pressure forces at the extremes of the needle.

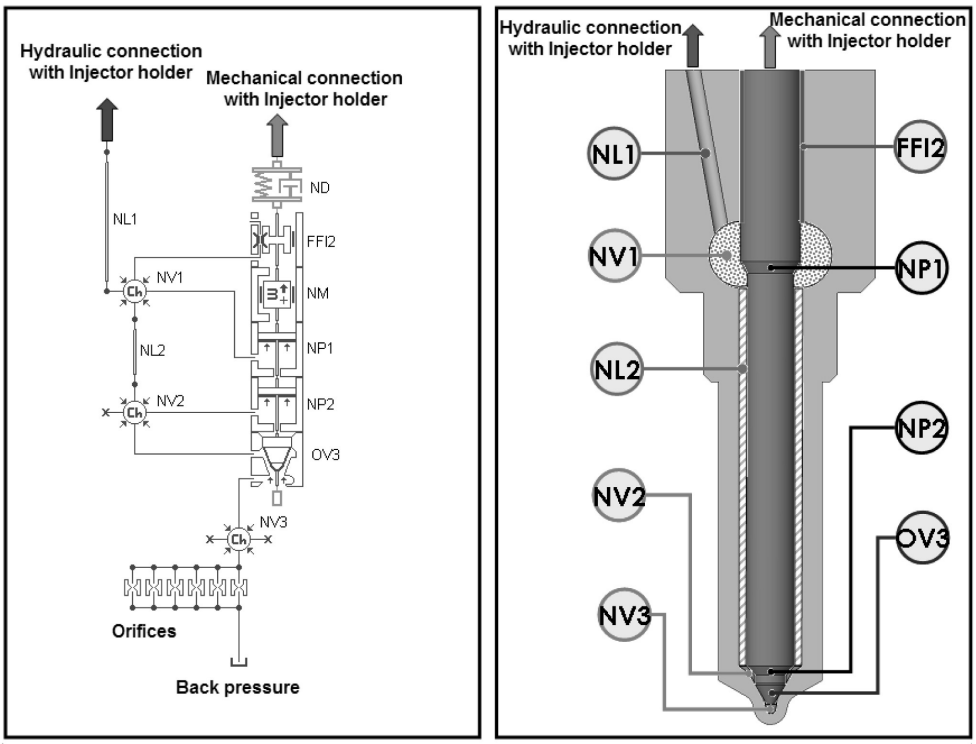

Fig. 3. Model of the nozzle (adapted from [13]).

As with the inlet and outlet orifices of the control volume, one of the most critical aspects for modeling the nozzle is the internal dimensions of the discharge orifices, as well as their hydraulic characterization. In this case, through the use of the silicone method, the most important dimensions of the needle seat can be found as well as the diameter of the orifices. From the point of view of the one-dimensional model, the most important parameters are the number of orifices and their respective diameters, since they define the permeability (discharge capacity) of the nozzle. The diameter of the five orifices was determined for the characterized nozzle. The mean value was 131 μm, with a standard deviation of ± 2 μm. Additional details about the nozzle model are available in [13].

2.3 Model of the electro-valve

Figure 4, top left, shows a physical sketch of the electro-valve and, top right, a zoom of the magnetic path is shown. The model created with the AMESim code is depicted below. The moving element of the electro-valve is the command piston, labeled AM in the figure. The ascending movement of the command piston due to the command electric current opens the outlet orifice of the control volume by displacing the small sphere. Therefore, the displacement signal of the command piston is the only connection that exists with the model of the injector holder. The spring BS opposes the opening of the control piston and maintains the piston and the small sphere closing the outlet as long as there is no excitation current.

The electro-valve is fed by a voltage signal that acts as an input of the variable voltage source (U). This signal is a reproduction of that provided by the Electronic Control Unit of the engine for a given energizing time of the injector. The voltage source is connected to an electric coil with 32 coils. The current in the electric circuit induces a flux in the magnetic circuit. The magnetic flux passes through the actuator core (MC1, MC2 and MC3), the upper part of the command piston (MC4 or IND-induced) and the air-gap (AG). Elements MC1 and MC3 are longitudinal magnetic elements, while elements MC2 and IND are radial magnetic elements. Their reluctances depend on the material. The lengths and effective magnetic areas have been estimated based on a dimensional analysis. Further details about the electro-valve model are available in [13].

3. Students' work in the practical lesson

In this section the work done by the students during the practical lesson will be described. The subsections will show the different tasks proposed, as well as the different aspects of the fuel injection system that the students are supposed to learn. This will

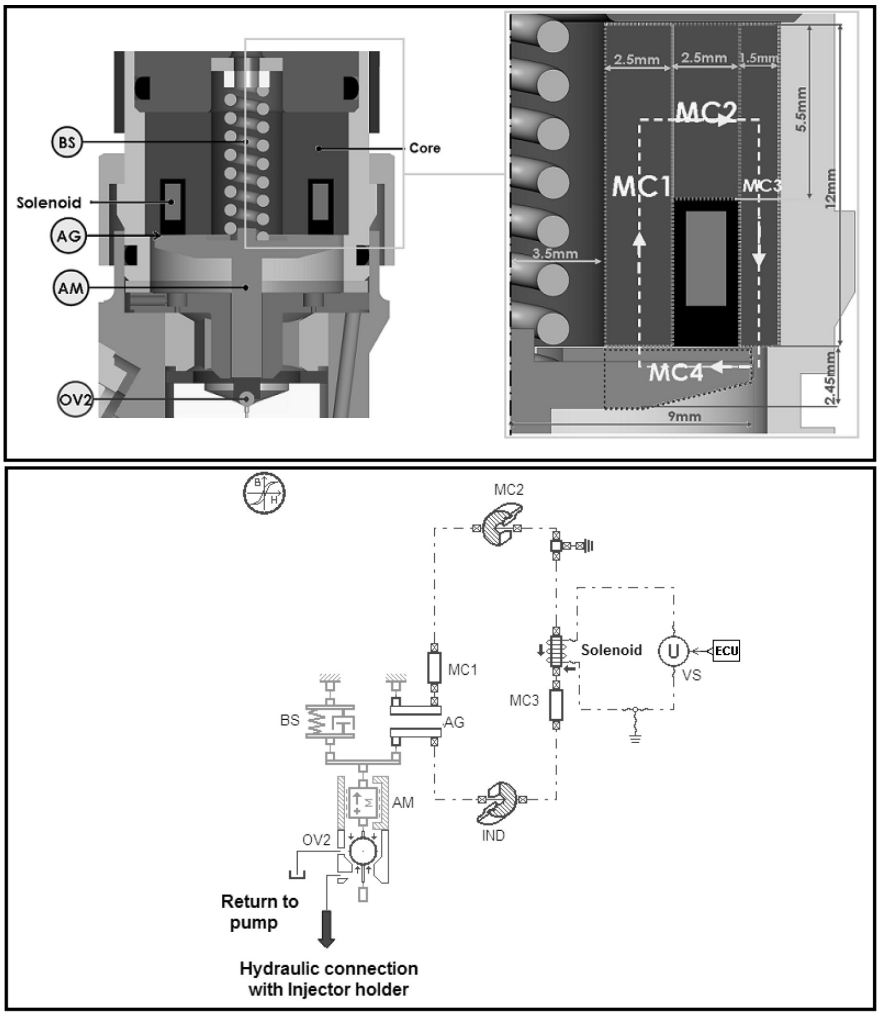

Fig. 4. Model of the electro-valve (adapted from [13]).

show the potential of the proposed methodology to fully understand in detail such a complex system.

3.1 Description of the main parameters of the system and test matrix definition for the students' work

For the analysis of the results, students are asked to simulate the points in Table 2. In this table, for simulations A, B and C, the same diameter for the nozzle orifices is used (equal to 0.23 mm). These simulated points differ only in the pressure in the rail. Students have to search the energizing time (duration of the electrical signal) in such a way that the total mass injected in the three cases is the same and equal to 32 mg per injection. In the last column of the table, the total injection duration (time period in which the needle is opened) have to be filled in by the students. The comparison of these simulations is expected to be useful for the students to understand the influence of the injection pressure on the injector dynamics.

Cases D and E differ from cases A, B and C in the different diameter of the nozzle orifices. In the case of simulation D, a larger diameter is used and students have to search for an injection pressure and energizing time in such a way that the total mass injected is the same as before (32 mg) and, as an additional restriction, the injection duration is the same as the reference case (simulation B). Obviously, a lower injection pressure than in case B is expected to be used for the students to fulfill both criteria.

Point E is similar to point D, but in this case the diameter of the nozzle orifices is smaller than in cases A, B and C. Again, the students are asked to search for an injection pressure and energizing time in such a way that the same total mass injected and injection duration as in case B are obtained. Obviously, in this case, a higher injection pressure than the reference case (B) is expected to be used for the students to satisfy those requirements.

An example of the results obtained by the students after their task is depicted in Table 3. They are

Table 1. Values of the main parameters of the model.

Control volume configuration:	
Diameter of control volume inlet orifice (orifice OZ in Fig. 2) [m]:	$270 \cdot 10^{-6}$
Diameter of control volume outlet orifice (orifice OA in Fig. 2) [m]	$300 \cdot 10^{-6}$
Injector nozzle configuration:	
Number of orifices [-]:	5
Diameter of nozzle orifices [m]:	From $190 \cdot 10^{-6}$ to $250 \cdot 10^{-6}$
Rail:	
Volume [m^3]:	25
Pressure in the rail [MPa]:	30 , 70 and 110
Combustion chamber:	
Pressure in the combustion chamber (backpressure) [MPa]:	2
Fuel Properties:	
Density [kg/m^3]:	820
Kinematic viscosity [m^2/s]:	$3.1 \cdot 10^{-6}$
Surface tension [kg/s^2]:	0.024

Table 2. Points to be simulated by the students using the AMESim model.

POINTS	Number × Diameter of nozzle orifices [mm]	Pressure in the Rail [MPa]	Total mass injected [mg/cc]	Energizing Time (ET [μs])	Injection Duration (Δt [μs])
A	5 × 0.23	30	32	—	—
B	5 × 0.23	70	32	—	Δt_B [μs]
C	5 × 0.23	110	32	—	—
D	5 × 0.25	—	32	—	Δt_B [μs]
E	5 × 0.19	—	32	—	Δt_B [μs]

Table 3. Results of the simulation performed by the students.

POINTS	Number × Diameter of nozzle orifices [mm]	Pressure in the Rail [MPa]	Total mass injected [mg/cc]	Energizing Time (ET [μs])	Injection Duration (Δt [μs])
A	5 × 0.23	30	32	**1290**	2040
B	5 × 0.23	70	32	**667**	1240
C	5 × 0.23	110	32	**500**	1000
D	5 × 0.25	**59**	32	**630**	1240
E	5 × 0.19	**112**	32	**750**	1240

asked to plot the mass flow rates provided by the model for all the cases. These mass flow rates are given in Fig. 5. The total mass injected (i.e. the integration over the time of the different curves, see e.g. case A, where this surface is marked) should be the same, and equal to 32 mg, for all five cases. Also, as imposed by the injection conditions of Table 2, the injection duration for cases B, D and E are the same.

3.2 Description and analysis of how the injector works

In this section the students are asked to describe and analyze how the injector works. They have to use the injection conditions and simulation results provided by the model for case C for their reasoning.

For this, students have to plot two different graphs like those represented in Fig. 6, where different internal variables that are essential to explain what is going on in the different parts of the injector have to be depicted.

The variables represented in the upper part of Fig. 6 are the pressure in the rail, the discharge pressure (fixed at a value of 2 MPa), the pressure in the control volume (V2 in Fig. 2), as well as the injection flow delivered to the combustion chamber and the control flow needed to operate the injector. This last flow is the flow passing through the orifices OZ and OA (Fig. 2) when the injector is under operation.

At the bottom of Fig. 6, students have to plot the mass flow rate (mass delivered to the combustion chamber), as well as the needle and the command piston lift laws as functions of time.

Analyzing the evolution of such variables, students have to provide a description of the different steps of the injector operation.

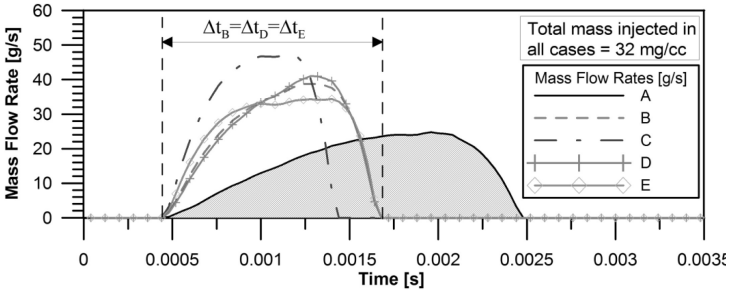

Fig. 5. Mass flow rates obtained for the different simulated cases.

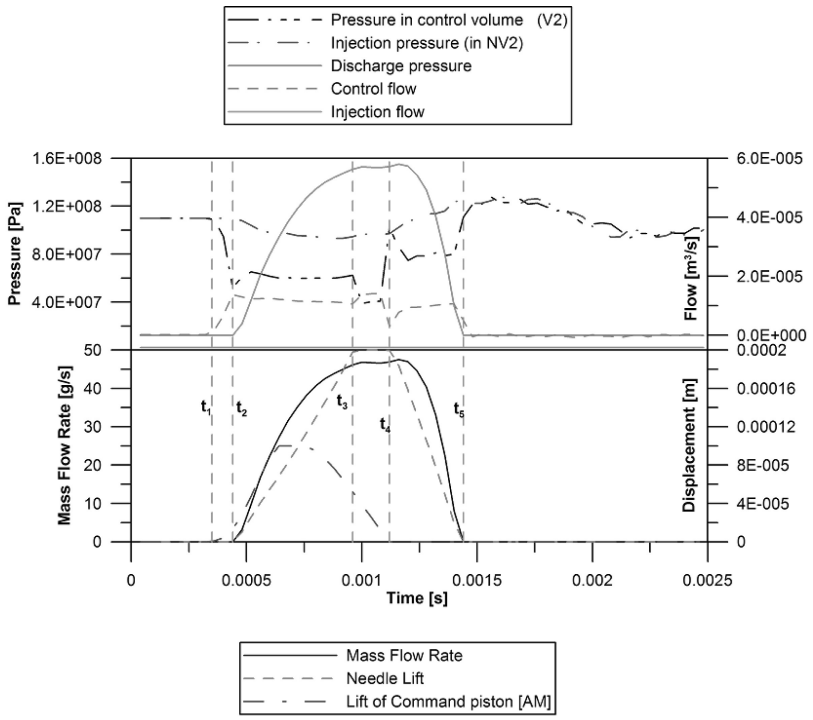

Fig. 6. Internal variables of the injector used for the injector behavior description.

Here, an example of the description that the students should provide is given:

- Under non-operative conditions, that is, without any electrical excitation, the nozzle needle remains on its seat, so the discharge orifices are blocked and, as a consequence, there is no injection. In this situation, as can be seen in the picture, the pressure acting on the upper surface of the rod and the pressure acting in the lower part of the needle are the same and equal to the pressure in the rail. Since the surface in the upper part of the rod is higher than that existing in the lower part of the needle, the resulting force keeps the needle down, closing the nozzle orifices.
- The start of the injection (time instant, t_1 in Fig. 6) is produced when, after the energizing of the injector, the command piston (AM in Fig. 4) opens the orifice OV2 (Fig. 2). The command piston lift law can be seen in the bottom part of Fig. 6. As a consequence, a flow is established (control flow), which passes through the orifices OZ and OA, among others parts. The inlet orifice of the control volume (OZ) produces a pressure loss that results in a decrease of the pressure within the volume V2. This pressure drop can be seen in the upper part of Fig. 5.
- As a consequence, and taking into account that the pressure acting on the lower part of the needle is the rail pressure, the needle (also the rod) goes up until the mechanical upper limit is reached, as can be seen in the bottom part of Fig. 6.
- It can be observed that when the needle starts going up (time instant t_2), three different things happen: the fuel delivery starts, the pressure in the control volume (V2) increases slightly and the

control flow decreases a little. All these phenomena are related to the diminution of the volume in the upper part of the rod due to the needle lift. The needle achieves the maximum lift at time instant, t_3.

- At time instant, t_4, when the energizing time finishes, the end of the injection starts. At this time instant, the command piston (AM in Fig. 4) closes the return line. As a consequence, the pressure in the control volume increases until it reaches the same pressure as in the rail. The increment of the pressure makes the force on the upper part of the rod, again, higher than that acting on the lower part of the needle. So, as a consequence, the needle starts going down. A decrease in the mass flow rate is clearly observed during this closing stage. Finally, the injection ends at time instant t_5, where the needle, as at the beginning, totally closes the discharge orifices.

It can be observed that these simulations are a powerful tool to fully understand the complex operation of a common rail injector.

3.3 Influence of rail pressure on the injector behavior

Students are asked in this section to compare, from the point of view of the system dynamics, the behavior of the system when the injection pressure changes.

Their answer should be based on the results of simulations A, B and C, where the injection pressure is varied, keeping the same diameter of the nozzle orifices.

To help the students to answer this question, they are asked to plot the needle lift law as a function of time for the simulated points A, B and C. As can be seen in Fig. 7, from the point of view of injector dynamics, as the injection pressure increases, the needle lift is faster (case C), whereas the needle movement becomes slower when the rail pressure takes lower values. Since the mass flow rate depends on needle dynamics, a direct consequence that can be established is that, when the injection pressure is lower (case A), a higher energizing time (and so, injection duration) is needed to inject the same total mass quantity, whereas the total injection time has to be reduced when the injection pressure increases (case C), to fulfill with the same total mass injected.

3.4 Analysis of needle lift velocities as a function of the rail pressure

In this section, students are asked to compare the needle lift velocities as a function of the injection pressure. To analyze this behavior they have to plot the needle velocity over time for the cases A, B and C. They have to obtain and describe a plot like that depicted in Fig. 8. In that figure, the velocity is represented as a function of time. A positive value for velocity indicates that the needle is going up, while a negative value for velocity indicates that the needle is going down. As can be seen, when the cases A, B and C are compared in the upper part of Fig. 8, the higher the injection pressure, the higher the velocity of the needle. The reason of this different behavior is found in the differences in pressure existing between the upper part of the rod and the bottom part of the needle when the three cases are compared. These differences can be easily observed in the upper part of Fig. 9 where the Delta P, defined as the difference of pressure between the upper part of the rod and the lower part of the needle, is represented as a function of the time for the three cases. As can be observed, for case A the difference is around 10 MPa, whereas in the case C, this difference is around 40 MPa. The velocity can be normalized by dividing for the rail pressure (Fig. 7, in the bottom). In this case, we can see how the normalized velocity is the same in all the cases, being only different in the final part of the injection according to the different energizing time used to obtain the same total mass injected. So, it is possible to conclude that the needle velocity is proportional to the rail pressure, which is, in fact, its driving force.

3.5 Injection pressure characteristics: pressure losses and dynamics effects

In this section the injection pressure is analyzed by the students. For that purpose, students are asked to

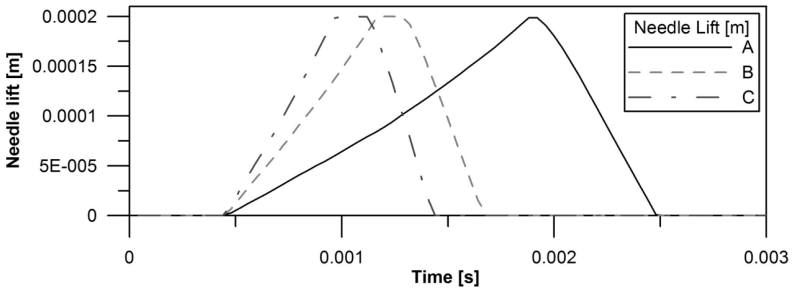

Fig. 7. Needle lift comparison for simulations A, B and C described in Table 2.

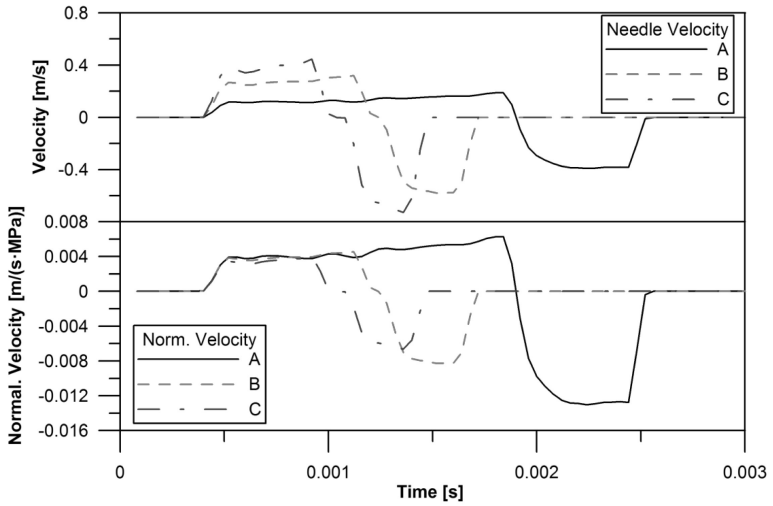

Fig. 8. Needle lift velocities as a function of the injection pressure (comparison for simulations A, B and C described in Table 2).

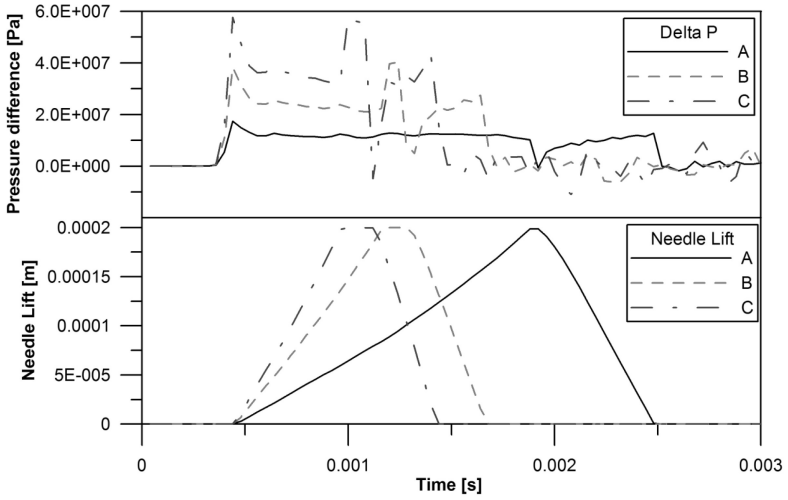

Fig. 9. Needle lift comparison for simulations A, B and C, which are described in Table 2.

explore the evolution of the pressure in volume NV2 in Fig. 3. This pressure depends on the rail pressure but it also takes into account the pressure losses along (a) the injector holder and (b) part of the nozzle (except the final conical seat and discharge orifices, which will be analyzed in the following subsection).

Students also have to reflect in their analysis on how this pressure is related to the control flow, the mass flow rate and the needle lift.

Taking case C as a reference, the students have to plot the injection flow, the injection pressure and the control flow, obtaining the graph depicted in Fig. 10.

In the figure, time instants, t_i, are the same as those defined previously in Section 3.2. From this figure, it can be observed that when the command piston (AM in Fig. 4) opens the orifice OV2 (in Fig. 2), the control flow starts appearing (instant t_1), and it reaches a first maximum value at t_2. Nevertheless, the injection pressure does not change during the time interval from t_1 to t_2. As stated in Section 3.2, the start of injection takes place in instant t_2 when the rod and needle start moving due to pressure differences between the upper part of the rod and the lower part of the needle. At this point there is a decrease in the injection pressure due to friction losses. It means that the injection pressure is mainly influenced by the injection flow rate, and so strongly depends on the needle lift, whereas it does not depend on the control flow. The minimum pressure is reached at t_3 when the injector is providing the maximum flow. After this time instant, the pressure waves generated at the beginning of the injection

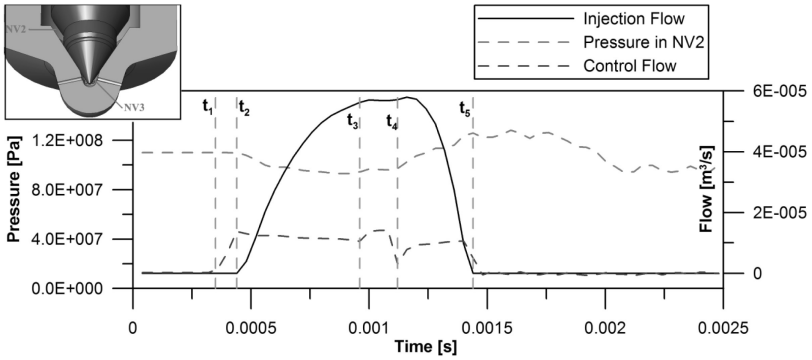

Fig. 10. Needle injection flow, injection pressure (in volume NV2) and control flow for case C in Table 2.

(which are traveling along the injector, from the nozzle tip to the rail and from there to the nozzle tip) start affecting the injection pressure, giving a sinusoidal character to the injection pressure signal, even further from the end of the injection (t_5).

After this first reasoning, students are asked to compare the injection pressure evolution as a function of the rail pressure. For that purpose, they have to plot the relative pressure as a function of time for cases A, B and C. They obtain a plot similar to that shown in the upper part of Fig. 11. In that figure, it is possible to see the "relative" injection pressure (in the volume NV2) for the different values of rail pressure (cases A, B and C). In this case, to allow the comparison, the rail pressure has been subtracted from the pressure signal in volume NV2. It can be observed that the most important variation in terms of amplitude is detected for the case with the higher rail pressure (case C), which is reasonable taking into account the higher mass flow rate injected for this case, and so the higher pressure losses affecting the pressure signal at volume NV2. Also, the amplitude of the residual oscillations that remain after the injection process becomes more important as the rail pressure gets higher values.

To completely remove the effect of the rail pressure, in the bottom part of Fig. 11, students are asked to plot the same information, but in this case, the relative injection pressure is divided by the initial rail pressure. It should be remarked that, for all the cases, the curves obtained are more similar, especially at the beginning where, for all the cases, the injector is in the opening phase. It demonstrates that pressure losses and pressure oscillations are proportional to the rail pressure at which the system is operating.

3.6 Effective injection pressure

In this section, the students are asked to compare the pressure at volume NV2 (evaluated in the previous subsection) and the effective injection pressure, just upstream of the nozzles discharge orifices. This pressure is the pressure existing inside the volume NV3 in Fig. 3. For this they

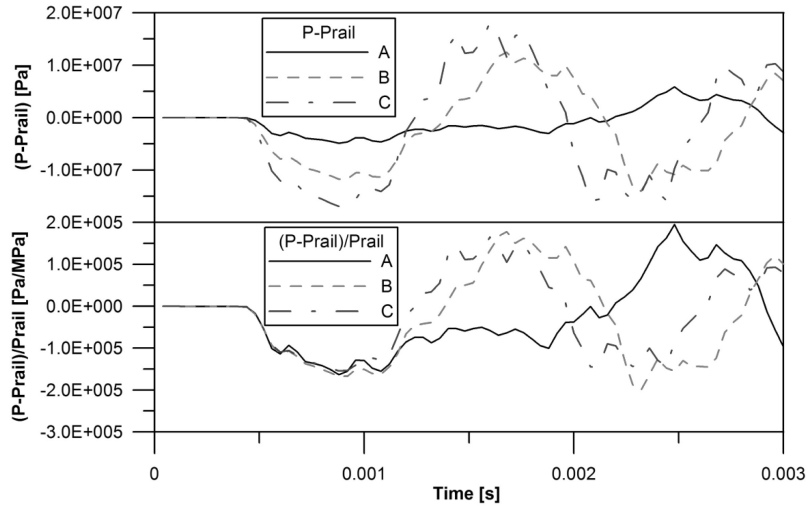

Fig. 11. Relative injection pressure for cases A, B and C defined in Table 2.

have to plot both pressures as functions of time for case C, obtaining a graph similar to that depicted in Fig. 12. In this figure, in order to explain the differences between both pressures, they also have to represent the needle lift as a function of time.

As stated, the pressure in volume NV2 is affected by the pressure losses, which depend mainly on the mass flow injected during the injection time interval, and by the pressure waves traveling through the main injector channel. These pressure waves, in particular, have an effect at the end of the injection, originating oscillations in the pressure. Nevertheless, as can be seen in Fig. 12, the pressure in NV3, which can be considered to be the effective injection pressure, behaves in a different way from the pressure in the volume NV2. Both volumes are physically separated by the needle and its seat, so the difference between both pressures is the pressure loss in the annular throttle passage formed between the needle and the seat. This section of passage depends strongly on the needle lift, and so the pressure losses expected at low needle lifts are higher than those expected at higher needle lifts. This behavior can easily be observed in Fig. 12. From the figure it can be seen that the pressure in volume NV3, at the beginning (before the injection event), is equal to the back pressure fixed in the discharge chamber, 2 MPa. Once the needle starts its motion (and so the injection event starts), the pressure in volume NV3 increases. As shown in the figure, the higher the needle lift, the higher the effective injection pressure. For a given instant, the difference between both pressure signals provided by the model represents the pressure losses in the needle seat. For the maximum needle lift, 200 μm, the difference between both pressures is minimum, being representative of the pressure losses that the needle throttle introduces even in the case where the flow is less perturbed in terms of wall friction.

3.7 Injection velocity

In this section the students are asked to represent the effective injection pressure for all the simulated cases, and to compare this pressure with the injection velocity. It is well known in the diesel engine researchers' community that the injection velocity is one of the most important parameters enhancing the air–fuel mixing process: the higher the injection velocity, the more efficient the air–fuel mixing process. Therefore, it would be important at this point of the practical session to determine and compare the effective injection velocities for all the cases in order to qualitatively compare the injection process from the point of view of the fuel–air interaction. Moreover, the prediction of the air–fuel mixing process will be a useful starting point in the following practical lesson that students have to perform during the topic. With the help of the model, they obtain the graph plotted in Fig. 13, where the effective pressure and the injection velocity provided by the model are depicted over time for all the simulated points. As can be seen, the shape of both types of curves is identical, a result that is reasonable if we take into account that the injection velocity depends on the squared root of the pressure difference upstream and downstream of the orifices. Since the discharge pressure is constant and equal to 2 MPa, the effective velocity should show the same behavior as the effective pressure. Nevertheless, as

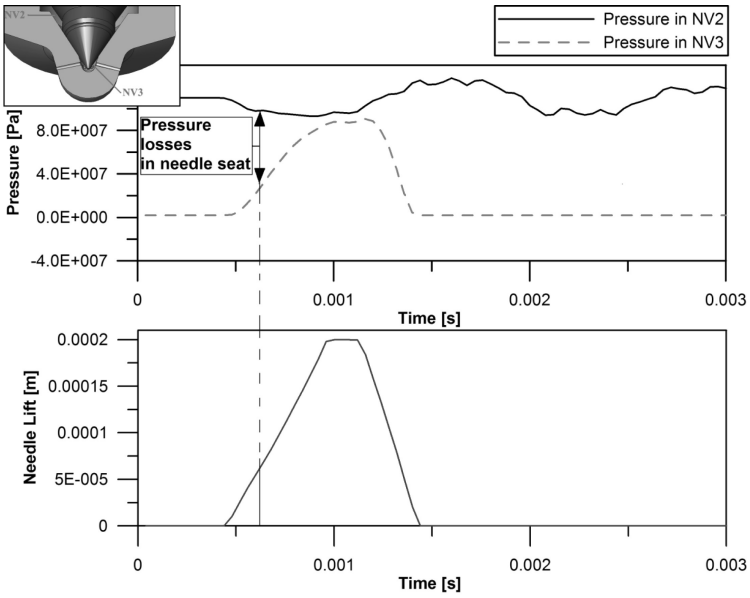

Fig. 12. Pressures in volumes NV2 and NV3. Comparison for case C in Table 2.

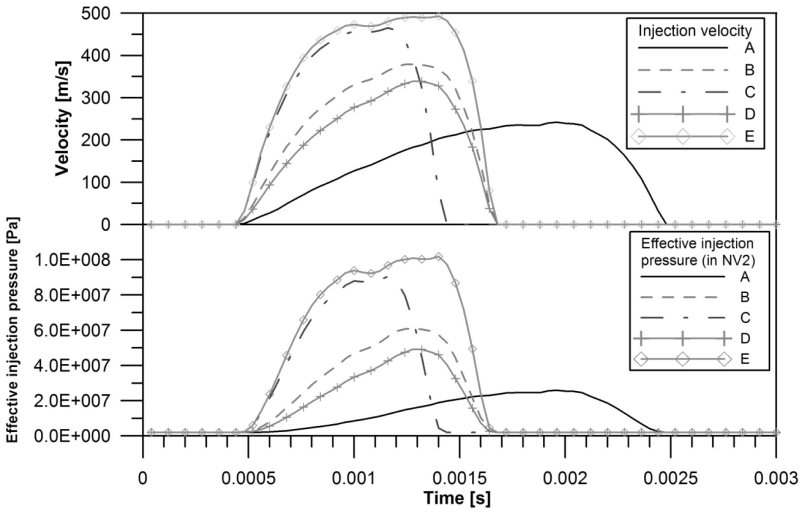

Fig. 13. Injection velocity and effective injection pressure for all the simulated cases.

can be observed in the figure, the velocity profile shows a more attenuated shape, since, as commented above, it depends on the square root of the pressure drop. As can be deduced from the figure, the higher the injection pressure, the higher the injection velocity. If we compare the different cases, the highest injection velocity belongs to case E, where a rail pressure of 112 MPa is used, and a maximum velocity close to 500 m/s is reached. On the other hand, case A is found to have the lowest injection velocity, with 30 MPa of rail pressure and a maximum velocity of 200 m/s. The other conditions show maximum velocities in the range defined by these two extreme cases, A and E.

3.8 Prediction of the diesel spray behavior and combustion process

In this last section the students are asked about the results of using the different fuel injection rates on the spray development and combustion process, taking into account that in every case the same fuel mass is injected.

From the lectures on the subject where this practical lesson is given, the students gain knowledge about the parameters that serve to predict the quality of the fuel–air mixing process and, therefore, the combustion efficiency. They know how important the velocity is in the mixing process [20, 21]. In overall terms, the higher the injection velocity, the better the mixing process and the faster the combustion process. Furthermore, it is also well known that using a nozzle with a small orifice diameter promotes the atomization process. Taking into account all these things, case E, with the highest injection velocity and the smallest nozzle diameter, probably would be the best of all cases.

4. Results of the new teaching methodology

The present practical lesson was introduced in the subject "Mixing formation and combustion systems in RICE" in the academic year 2008–2009, when it was going to be taught for the second time. Consequently, the results of the new teaching methodology can only be compared with the results of one year (academic year 2007–2008).

To begin with, it is worth noting that the assessment of any teaching methodology is not an easy task, and research in this field has recently increased [1]. At UPV it is common to evaluate the different teaching activities using an opinion poll taken from the students involved in the corresponding activity. As stated by [22], though it is not the best way, most engineering education researchers prefer a quantitative methodology for evaluation, and that also applies to students' evaluations of the teaching methodologies. The average grading of the present workshop with the previous teaching methodology was 7.2 over 10, whereas it is 8.5 over 10 with the new methodology (average of three academic years). This result shows that the student considers the new methodology as being more suitable to the understanding of the operation of modern common rail injection systems. Another proof of the suitability of the new methodology is found when this practical lesson is compared with a similar one performed by undergraduate Mechanical Engineering students. In this case the practical session is based on a detailed explanation of how the common rail injection system operates, supported by a video. In addition, the student can see and touch the different parts of one such system. In this practical

session, the average grading given by the students is 7 over 10 (average of 5 academic years).

Besides this "quantitative" evidence, the teachers making use of this new methodology have observed that the students gain a deeper knowledge of how the common rail injection system operates, as they are able to explain this operation when they are asked, thus giving further (in this case "qualitative") evidence of the suitability of the new methodology.

A final remark is that it is strongly recommended that the presented simulation tool is not used as the only way to present the student with the common rail injection system. The students also need to see a real system, with its different components, to have a realistic idea in mind of the system they are simulating. This is, in fact, a usual limitation of computer-based teaching activities.

5. Conclusions

In this paper, an alternative methodology for teaching how modern common rail injection systems work has been defined and compared with the previous methodology. The new methodology is based on the use of a one-dimensional injector model that had previously been validated. It is not an easy task to validate an injector model, but thanks to previous experience at the CMT-Motores Térmicos research institute, this solenoid operated injector was modeled with high accuracy. Only some of the details of the model are presented in this paper, but the complete details of the model are available in the literature so that other teaching institutions could reproduce the practical lesson presented here.

The work that the students are asked to do with the model, and the detailed information that they can obtain from the model allow them to gain a deep understanding of the solenoid operated injector used in current common rail systems. This shows the strong potential of such tools for educational purposes. At the end of the practical session the students have an insight into how the injector operates, and also get an idea of how the injection pressure and the nozzle diameter are related to each other.

Finally, the improvement in the teaching methodology of this practical lesson has been demonstrated "quantitatively" by its average grading based on an opinion poll taken from among the students, ranging from 7.2 over 10 with the former methodology to 8.5 over 10 with the new one. The improvement has also been demonstrated "qualitatively" as the teachers making use of this new methodology have observed that the students gained a deeper knowledge of how the common rail injection system operates, as they were able to explain this operation when asked.

References

1. B. K. Jesiek, M. Borrego, K. Beddoes, M. Hurtado, P. Rajendran and D. Sangam, Mapping global trends in engineering education research, 2005–2008, *International Journal of Engineering Education*, **27**(1), 2011, pp. 77–90.
2. H. Ku and R. Fulcher, Using computer software packages to enhance the teaching in engineering management science – Part 2: Programming techniques, *Computer Applications in Engineering Education*, **20**(1), 2012, pp. 114–123.
3. J. Magana, S. P. Brophy and G. M. Bodner, Student views of engineering professors technological pedagogical content knowledge for integrating computational simulation tools in nanoscale science and engineering, *International Journal of Engineering Education*, **25**(5), 2012, pp. 1033–1045.
4. C. Gencer and M. Gedikpinar, A computer-aided educational tool for induction motors, Computer Applications in Engineering Education, **20**(3), 2012, pp. 503–509.
5. M. Zheng and R. Kumar, Implementation of multiple-pulse injection strategies to enhance the homogeneity for simultaneous low-NOx and -shoot diesel combustion, *Int. J. Therm. Sci.*, **48**, 2009, pp. 1829–1841.
6. M. Yao, H. Wang, Z. Zheng and Y. Yue, Experimental study of n-butanol additive and multi-injection on HD diesel engine performance and emissions, *Fuel*, **89**, 2010, pp. 2191–2201.
7. H. K. Suh, S. H. Yoon and C. S. Lee, Effect of multiple injection strategies on the spray atomization and reduction of exhaust emissions in a compression ignition engine fueled with Dimethyl Ether (DME), *Energ. Fuel*, **24**, 2010, pp. 1323–1332.
8. J. M. Desantes, J. Arrègle and P. Rodríguez, Computational model for simulation of diesel injection systems, *SAE Paper 1999-01-0915*, 1999.
9. V. Amoia, A. Ficarella, D. Laforgia, S. De Matthaeis and C. Genco, A theoretical code to simulate the behavior of an electro-injector for diesel engines and parametric analysis, *SAE Paper 970349*, 1997.
10. A. Ficarella, D. Laforgia and V. Landrsicina, Evaluation of instability phenomena in a common rail injection system for high speed diesel engines, *SAE Paper 1999-01-0192*, 1999.
11. G. Augugliaro, G. Bella, V. Rocco, T. Baritaud and D. Verhoeven, A simulation model for a high pressure injection systems, *SAE Paper 971595*, 1997.
12. A-G. Favennec and M. Lebrun. Models for injector nozzles. *The six Scandinavian International Conference on Fluid Power, SICF' 99*, Tampere, Finland, May 26–28, 1999.
13. R. Payri, F. J. Salvador, P. Martí-Aldaraví and J. Martínez-López, Using one-dimensional modeling to analyze the influence of the use of biodiesels on the dynamic behavior of solenoid-operated injectors in common rail systems: detailed injection system model, *Energ. Convers. Manage.*, **54**, 2012, pp. 90–99.
14. F. Boudy and P. Seers, Impact of physical properties of biodiesel on the injection process in a common-rail direct injection system, *Energ. Convers. Manage.*, **50**, 2009, pp. 2905–2912.
15. R. Payri, H. Climent, F. J. Salvador and A-G. Favennec, Diesel injection system modeling. Methodology and application for a first-generation common rail system, *Proc. Instn Mech. Engrs (Part D: J. Automobile Engineering)*, **218**, 2004, pp. 81–91.
16. A. L. Boehman, D. Morris, J. Szybist and E. Esen, The impact of the bulk modulus of diesel fuels on fuel injection timing, *Energ. Fuel*, **18**(6), 2004, pp. 1877–1882.
17. H. K. Lee, M. F. Rusell and C. S. Bae, Development of cavitation and enhanced injector models for diesel fuel injection system simulation, *Proc. Inst. Mech. Engrs, (Part D, J. automobile engineering)*, **216**, 2002, pp. 607–618.
18. H. K. Lee, M. F. Rusell and C. S. Bae, Mathematical model of diesel fuel injection equipment incorporating non-linear

fuel injection, *Proc. Inst. Mech. Engrs, (Part D, J. automobile engineering)*, **216**, 2002, pp. 191–204.
19. LMS Imagine.Lab AMESim v.11, *User's manual*, 2011.
20. J. M. Desantes, R. Payri, F. J. Salvador and A. Gil, Development and validation of a theoretical model for diesel spray penetration, *Fuel*, **85**, 2006, pp. 910–917.
21. R. Payri, F. J. Salvador, J. Gimeno and V. Soare, Determination of diesel spray characteristics in real engine in-cylinder air density and pressure conditions, *Journal of Mechanical Science and Technology*, **19**(11), 2005, pp. 2040–2052.
22. M. Borrego, E. P Douglas and C. T. Amelink, Quantitative, qualitative, and mixed research methods in engineering education, *Journal of Engineering Education*, **98**(1), 2009, pp. 53–66.

R. Payri graduated in Mechanical Engineering in 1995, and received his Ph.D. in Mechanical Engineering in 1999 from the CMT-Motores Térmicos (Thermal Engines), Universitat Politècnica de València, Spain, where he has been a professor since 2000. Over the last ten years he has coordinated and participated in 40 competitive projects funded by European Union and national administrations, and more than 65 R&D projects funded by the industry. He has published 45 articles in international journals and 40 papers at international and national conferences. He has been supervisor of six doctoral theses. Currently Professor R. Payri is the head of the injection research group at CMT-Motores Térmicos.

J. Javier López received his Ph.D. in Mechanical Engineering in 2003 at the Universitat Politècnica de València, Spain. He has been Assistant Professor since 1999, and from 2009 he has been Associate Professor at CMT-Motores Térmicos. His teaching focuses on thermodynamics, heat transfer, and thermal machines and engines, mainly for mechanical engineers. His research is focused on the injection/combustion process in direct injection diesel engines. He has collaborated in the publication of three lecturer books, and more than twenty articles for international scientific journals and conferences.

F. J. Salvador graduated in Mechanical Engineering in 1998 and received his Ph.D. in Mechanical Engineering in 2003 from the Universitat Politècnica de València, Spain. He has been Associated Professor since 2005 at CMT-Motores Térmicos. His teaching focuses on thermal machines and engines. His research focuses on the injection process in direct injection diesel engines. Over the last ten years he has coordinated and participated in more than twenty competitive projects funded by European Union and National administrations and more than 40 R&D projects funded by the industry. He has published 40 articles in international journals included in the journal citation reports and more than 30 papers at international and national conferences. He has supervised three doctoral theses.

P. Martí-Aldaraví is a Ph.D. student and has been Assistant Professor of Aerospace Engineering at CMT-Motores Térmicos since 2010. He received his BS and Master in Aerospace Engineering at the Universitat Politècnica de València, Spain. Currently his research is based on numerical simulation of the diesel injection system considering both internal and external flows.